Ultraviolet surface-emitted second-harmonic generation in GaN one-dimensional photonic crystal slabs

J. Torres, M. Le Vassor d'Yerville, D. Coquillat, E. Centeno, and J. P. Albert
Groupe d'Etude des Semiconducteurs-UMR 5650, CNRS Université Montpellier II, 34095 Montpellier Cedex 5, France
(Received 3 December 2004; revised manuscript received 1 February 2005; published 26 May 2005)

We report on the observation of an exalted second-harmonic generation process related to a resonant effect inside a GaN photonic crystal slab. The measured enhancement factor, close to 10^4, is the highest measured in this photonic crystal slab resonant configuration. This frequency conversion process is also successfully compared to a rigorous modeling using a scattering matrix formalism. In addition, an original polarization study is proposed, leading to an evaluation of the relative contributions of the fundamental and the second-harmonic modes resonances in the second-harmonic response magnitude.

DOI: 10.1103/PhysRevB.71.195326 PACS number(s): 42.70.Qs, 42.65.Ky, 78.66.Fd

Photonic crystals (PCs) are periodically textured structures exhibiting remarkable optical properties related to the strong perturbation of their electromagnetic dispersion curves.[1,2] Among those properties, the most commonly mentioned is the emergence of frequency ranges called photonic band gaps inside which the propagation of light is forbidden. This band gap effect offers the attractive possibility to control the propagation of light through the introduction of defects inside the periodic photonic lattice. However, in addition to photonic band gaps, the high index contrast of the modulated slab is also responsible for a strong modification of the allowed bands. This is also of great interest since it generates high density of states regions, lying especially close to the band gaps. Inside these regions, an enhanced optical response of the PC slab is generally observed, and is associated with a strong concentration of the photonic modes energy inside small volumes. Within this framework, noticeable improvements of nonlinear optical properties has been demonstrated inside various PC structures.[3–8]

PC slabs are periodically etched films with a finite height providing a vertical confinement of electromagnetic modes by total internal reflection. However, most of the photonic modes are only partially confined inside the slab because of a diffractivelike coupling with the radiative continuum of the surrounding medium. These modes are then characterized by a finite lifetime inside the slab and suffer intrinsic vertical losses during their propagation inside the PC slab. This may severely limit the applicability of PC inside photonic integrated optical circuits.[9,10] Recently, PC slab structures have nevertheless been proposed to be used as efficient vertical resonant cavities.[11] In this context, the diffractive external coupling process plays a positive role. First it allows injecting light inside the slab using a free standing wave impinging on the top surface of the textured slab. Inversely it is an excellent way to collect the enhanced light signal emitted from the surface, after the resonant interaction within the optically active slab material. This resonance phenomenon, associated to the strong energy localization of the PC modes, significantly enhances light-matter interaction. It can then be efficiently exploited in order to intensify nonlinear frequency conversion processes.[12] Such a resonantlike exaltation of optical nonlinear effects is similar to the "guided-wave resonance" effect studied by Reinisch and Nevière inside guiding structures consisting of a homogeneous slab lying under a grating coupler.[13] On the other hand, it is worth noting here that this frequency conversion enhancement within vertical resonance conditions differs fundamentally from the technique provided by "nonlinear photonic crystal"[14] relying on a periodic inversion of the second-order susceptibility tensor $\chi^{(2)}$. The resonantly enhanced frequency conversion process was first proposed inside etched PC slab structures by Cowan *et al.*[15] with theoretically predicted enhancement factors as high as 10^6 inside GaAs structures. Consecutively, experimental demonstrations of enhanced second-harmonic generation (SHG) have been performed inside GaAs planar PCs.[16,17]

In this work, we report on the experimental demonstration of a giant SHG process inside a GaN 1D PC slab. GaN-based structures have already proven a massive impact on photonics and optoelectronics. Here they provide new possibilities concerning frequency conversion processes. The main improvement using GaN instead of GaAs lies in the ability to convert light from infrared to ultraviolet because of a wide transmission range from 365 nm to 13.5 μm. Despite GaN nonlinear second-order susceptibility $\chi^{(2)}$ is about 10 times lower than in GaAs, it is expected to be enhanced in the presence of internal piezoelectric fields induced by quantum wells.[18] In this case, non-linear coefficients could be as high as inside GaAs. GaN also exhibits a high optical damage threshold[19] and a good mechanical ruggedness.

The sample studied here consists of a 260 nm thick bulk GaN layer grown on the [0001] face of a sapphire substrate[20] and etched to obtain a succession of air stripes with a periodicity of 500 nm (see Fig. 1). The air filling factor and the stripes depth have been estimated to the respective values of 20% and 230 nm, by comparing the experimental band structure to the numerical one.[21] The resonant SHG process follows the subsequent description: an incident radiation first impinges on the above surface of the PC slab with a plane of incidence perpendicular to the air stripes (ΓX direction). This incident radiation is characterized by its frequency ω and in-plane wave vector $\mathbf{k}_{\|}$. Inside the GaN part of the slab, the second-order induced polarization $\mathbf{P}_{2\omega}^{\mathrm{NL}}=\varepsilon_0\chi^{(2)}:\mathbf{E}(\omega)\mathbf{E}^*(\omega)$ [where $\mathbf{E}(\omega)$ is the fundamental electric field] generates a

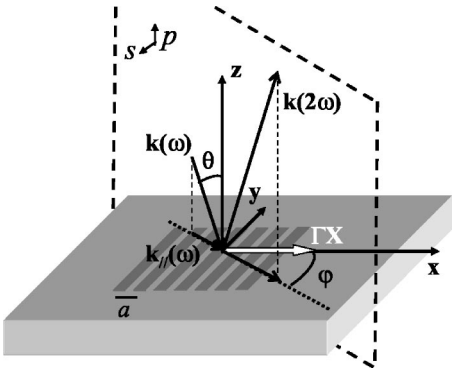

FIG. 1. Schematic representation of the 1D PC slab surface excited by an incident beam. a is the period of the photonic lattice, and θ and φ are, respectively, the incident and azimuth angles. $\mathbf{k}(\omega)$ is the wave vector of the incident beam, $\mathbf{k}_{\|}(\omega)$ is the in-plane component, and $\mathbf{k}(2\omega)$ is the wave vector of the radiated SH signal.

second-harmonic (SH) wave at 2ω which is reemitted from the surface in the surrounding vacuum. In this work, we only consider the 0th-order diffracted SH wave, so that this outgoing wave is characterized by the in-plane wave vector $2\mathbf{k}_{\|}$. With a uniform GaN slab, the frequency conversion process would remain limited by the refractive index dispersion of the material which induces a phase mismatch between the fundamental and SH interacting waves. The enhancement of the SHG process is here provided by the coupling with the PC resonant modes allowed by the folding of the photonic bands due to the periodicity. In this case, different exaltation situations with unequal effects exist. First, when the frequency ω and the in-plane wave vector $\mathbf{k}_{\|}$ of the incident wave match the frequency and the Bloch wave vector of a resonant PC mode, the fundamental EM field is strongly confined within the PC core, inducing a significantly enhanced source of SHG. Secondly, the SH field can also match a resonant mode of the PC slab at $(2\omega, 2\mathbf{k}_{\|})$ which can be efficiently coupled back in the surrounding vacuum. The third situation relies on the simultaneous fulfillment of both previous resonance conditions, and results in an optimized nonlinear conversion. These three situations will be respectively called resonant-nonresonant (RNR), nonresonant-resonant (NRR), and resonant-resonant (RR) conditions. In the last case, the coincidence of the resonances is fully related to the periodicity of the refractive index and the resulting folding and mixing of the bands inside the first Brillouin zone, which involves inside the PC the fulfilment of the equality $2\mathbf{k}_{\|}=\mathbf{k}_{\|}+\mathbf{G}$, via a reciprocal lattice vector $\mathbf{G}$. For this reason, the RR condition is also often called a "quasiphase matching" condition.[15] The relative impact of the RNR, NRR, and RR situations on the nonlinear process magnitude is worth to be evaluated.

In order to highlight the occurrences of enhanced nonlinear response and their relation with resonances inside the PC slab, we first give results obtained by extending the linear scattering matrix formalism[10,22] to the nonlinear response calculation. The solving of Maxwell equations is made assuming the fundamental EM field unperturbed by the SHG process. This is the undepleted pump approximation which is justified by low-efficiency conversion rates. Within this approximation, the calculation procedure[24] is simplified, as Maxwell equation at ω (fundamental frequency) and 2ω can be separately and successively treated.[23] In a first step calculation, Maxwell's equations at the fundamental frequency ω are solved, which leads to the determination of the electric field distribution produced by the incident wave inside the nonlinear GaN material. In a second step, the induced nonlinear polarization is determined from the fundamental electric field, and is treated as a source term inside Maxwell's equations solved at 2ω. This modeling takes into account the refractive index dispersion for GaN ($n=2.35$ for the fundamental wavelength, $n=2.55$ for the SH half wavelength). The induced polarization inside the GaN material (symmetry group $6mm$) is taken as[25,26]

$$\mathbf{P}_x(2\omega) = 2\varepsilon_0 d_{15} E_x(\omega) E_z(\omega),$$

$$\mathbf{P}_y(2\omega) = 2\varepsilon_0 d_{15} E_y(\omega) E_z(\omega),$$

$$\mathbf{P}_z(2\omega) = \varepsilon_0 d_{31}[E_x(\omega)^2 + E_y(\omega)^2] + \varepsilon_0 d_{33} E_z(\omega)^2 \qquad (1)$$

with $d_{15}=d_{31}=d_{33}/2=5.5$ pm/V. The in-plane isotropic distribution of the susceptibility tensor of the GaN layer is due to the alignment of the GaN crystal c axis with the z direction.

The lower graphs in Fig. 2 show, for two fixed values of $k_{\|}$ ($k_{\|}a/2\pi=0.190$ and $k_{\|}a/2\pi=0.158$), the radiated second harmonic intensity normalized against the intensity generated from the equivalent untextured GaN layer. This normalization procedure is used in order to isolate the PC role. Obvious enhancements of the SHG process are observed and can be clearly attributed to resonances of the fundamental and/or the SH modes of the photonic lattice. This is confirmed by the calculated transmission spectra reported above each diagram, showing the linear response of the slab to a p-polarized incident radiation around both the fundamental (filled circles) and the SH (empty circles) frequencies. These spectra are calculated using again a linear scattering matrix treatment,[22] and they bear out the emergence of Fano-like peaks occurring when the incident wave couples with a resonant mode of the slab. The resonant modes of interest here are labeled $2p$ and $5p$, according to the number of the corresponding photonic band and the polarization of the matching incident wave. The $3p'$ mode appearing in SH spectra is a second order mode and will not be used here. Figure 2(a) deals with NRR and RNR situations and the relative observed enhancements are coherent with a stronger influence of the resonance of the fundamental mode, compared to the resonance of the generated SH mode. In addition to the fact that other parameters such as the quality factors of the resonances have an influence on the enhancement factors, this is usually the case since the SH intensity has a square dependence on the fundamental field intensity.[27] In Fig. 2(b), the calculated SHG generation highlights a maximal and giant enhancement of the SH intensity by a factor 4.5×10^6. This corresponds to the achievement of an RR condition, which is confirmed by the overlapping of the Fano peaks of the modes $2p$ and $5p$.

For a global insight of the SHG process in the GaN PC slab, Fig. 3(a) gives a 3D plot of the normalized SH response

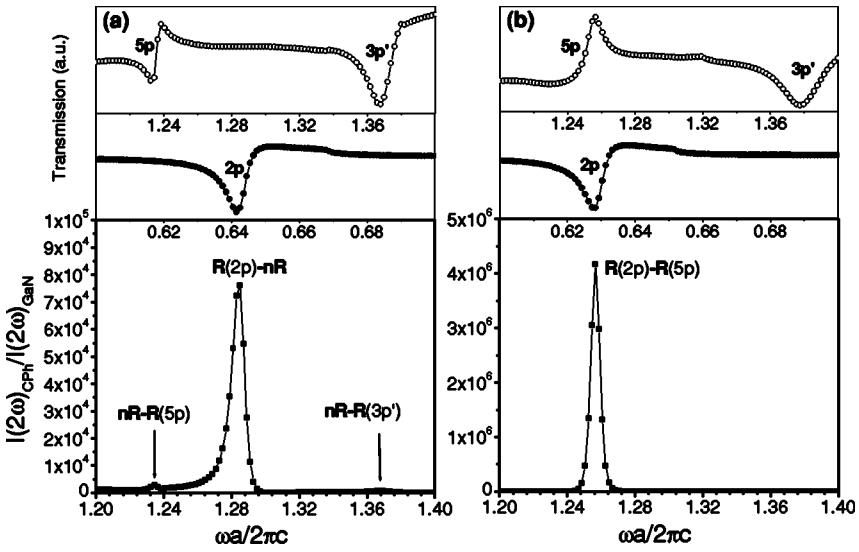

FIG. 2. Calculated normalized SH signal generated by the PC for fixed values of the in-plane wave vector, as a function of the radiated SH normalized frequency. The incident radiation is *p* polarized and the in plane wave vector is (a) $k_{\|}a/2\pi=0.190$ and (b) $k_{\|}a/2\pi=0.158$. Above are reported the corresponding linearly calculated transmission spectra at fundamental (filled circles) and SH frequency (empty circles).

as a function of the normalized frequency $\omega a/2\pi c$ and of the in-plane wave vector $k_{\|}$ along the ΓX direction. Figure 3(b) represents an upper view of the SH response in a grey (color online) logarithmic scale. The lines superimposed on this map are the dispersion curves of the fundamental mode (solid line) and the SH mode (dashed line) which are obtained by the scattering matrix poles calculation. The advantage of the poles determination is that it allows us a more precise and direct calculation of the intrinsic properties of the resonant modes of the slab.[10,23] The giant SH peak in Fig. 3(b) is clearly associated to the crossing of the calculated dispersion curves: this corresponds to the fulfillment of the RR condition, and results in a maximal enhancement factor close to 5×10^6. The single resonance conditions of both the 2*p* and 5*p* modes result in weaker enhanced peaks following exactly the corresponding photonic dispersion curves.

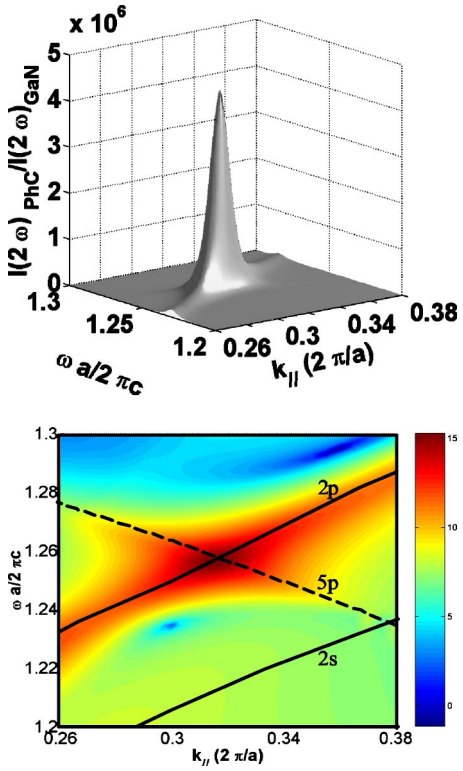

FIG. 3. (a) 3D insight of the numerical calculation of the normalized SH field intensity generated by the 1D PC along the Γ-*X* direction. The *x* axis is the incident wave vector in $2\pi/a$ units whereas the *y* axis is the normalized frequency. (b) Photonic band structure of the 1D PC superimposed on the grey (color online) scaled map of the SHG response of the slab. The solid line represents the photonic mode dispersion curves at fundamental frequency plotted at twice of their in-plane wave-vectors and frequency whereas the dotted line represents the 5*p* mode dispersion.

The above calculation procedure has demonstrated the existence of a RR condition occurring for a normalized frequency of 0.629 (wavelength 795 nm) and an in-plane component of the wave vector $k_{\|}a/2\pi=0.158$ (angle of incidence $\theta=14.6°$). The experimental demonstration of this giant SHG (the setup is described in Ref. 15) has been performed along the following lines: a *p*-polarized incident wave produced by a femtosecond laser beam at a fixed wavelength $\lambda=791$ nm impinges on the upper surface of the sample. In this setup, we suppose that the finite diameter of the beam does not cancel the role of the periodicity, as it covers about 80 periods of the PC. This fundamental incident wave generates a detectable SH radiated signal in the near UV (395 nm) which is detected from the above surface in a reflectionlike configuration. For the convenience of the procedure, the angle of incidence is fixed ($\theta=14°$) in order to avoid the realignment of the detection system that would be needed for each θ value. The evolution of the nonlinear optical response of the sample is nevertheless studied as a function of the azimuth angle φ in order to highlight the SH field enhancement related to the achievement of the RR condition (Fig. 4). As in the numerical study, the intensity of the measured SH field generated by the PC slab is normalized against the intensity of the SH field generated by an unpatterned zone of the GaN sample. The experimental peak related to the RR condition reaches a 7500 times enhancement. This experimental result validates the previous modeling predictions. The discrepancies between the SH intensity exaltation experimentally measured and calculated are mainly attributed to the nonverticality of the stripe sidewalls, which decreases the vertical

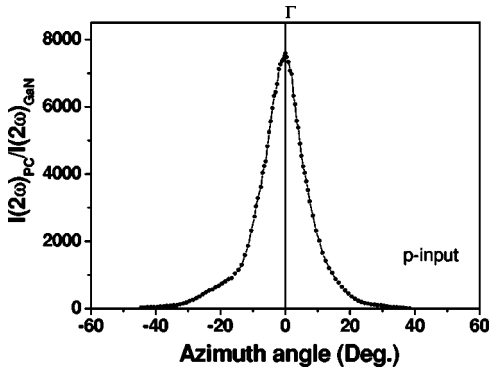

FIG. 4. Experimental azimuth variation of the normalized SH field intensity at $\lambda_{fund}=791$ nm. Filled circles denote SH light generated by a *p*-polarized pump field at $\theta=14°$.

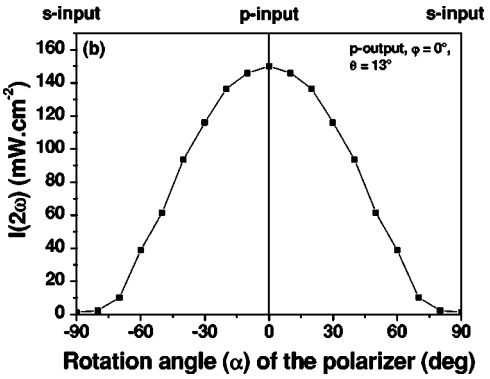

FIG. 5. Intensity of the *p*-polarized second harmonic generated in the 1D GaN PhC at 791 nm and for $\theta=14°$ as a function of the polarization angle α of the fundamental beam, with an incident plane along the ΓX direction ($\varphi=0°$).

quality factors of the resonances. This reduces the modes lifetime inside the nonlinear medium, and consequently the effects of light-matter interaction.

In order to better understand the relative contribution of each resonant coupling (at ω and 2ω) in the SHG process, we have also experimentally examined the dependence of the SH signal intensity on the polarization angle of the incident beam. Starting from the RR conditions, the polarization of the pump was tuned from *p* to *s* polarization using a Babinet-Soleil compensator. The results are shown in Fig. 5. When the incident beam is *p* polarized ($\alpha=0$) we observe, as expected, the maximum SH signal. When the incident beam is *s* polarized ($\alpha=90°$), no resonant mode is excited at the fundamental frequency, and the SH signal is divided by a factor 120. For the unpatterned GaN layer under equivalent illumination conditions, the decrease is only by a factor 4. We can then deduce that coupling simultaneously the fundamental field to the photonic mode $2p$ and the SH field to $5p$ (*p*-input-*p*-output configuration) is 30 times more efficient than coupling only to the SH field to $5p$ (NRR condition).

We have proposed in this paper a theoretical and experimental study of an efficient situation for the SHG process in a GaN PC slab. In the RR configuration explored here, a high enhancement of the SHG process is observed. The enhancement factor of 7500 is higher than the one measured before on the same sample.[21] The prevailing role of the confinement of the fundamental EM field is moreover demonstrated using a continuous variation of the incident beam polarization. A successful comparison is found between the theoretical predictions and the experimental occurrence of the RR condition. These tools then constitute a powerful means for a further optimization of the PC aiming at optimizing the SH response intensity. They will in particular allow studying the influence of all the photonic structure parameters or the intrinsic characteristics of the resonant modes such as their vertical quality factor or the overlapping of the spatial energy distribution of the fundamental and SH modes. The anisotropy of such PC structures have not been considered here but it allows preserving the same RR condition on a wide range of wavelength. This should give rise to new opportunities such as the possibility to provide compact tuneable solid-state lasers. Furthermore, the same approach could be used in more general nonlinear cases, such as third-harmonic and parametric conversion.

The authors would like to acknowledge Olivier Briot, Sandra Ruffenach, and Roger Aulombard for the growth of GaN epitaxial layers, and David Peyrade and Yong Chen of the Laboratoire de Photonique et des Nanostructures UPR 20, for the fabrication of the PCs. Professor Didier Felbacq and David Cassagne are also gratefully acknowledged for various helpful suggestions.

[1] E. Yablonovitch, Phys. Rev. Lett. **58**, 2059 (1987).
[2] S. John, Phys. Rev. Lett. **58**, 2486 (1987).
[3] J. Martorell and R. Corbalan, Opt. Commun. **108**, 319 (1994).
[4] J. Trull, R. Vilaseca, J. Martorell, and R. Corbalan, Opt. Lett. **20**, 1746 (1995).
[5] J. Martorell, R. Vilaseca, and R. Corbalan, Appl. Phys. Lett. **70**, 702 (1997).
[6] M. Scalora, M. J. Bloemer, A. S. Pethel, J. P. Dowling, C. M. Bowden, and A. S. Manka, J. Appl. Phys. **83**, 2377 (1998).
[7] M. Centini, C. Sibilia, M. Scalora, G. D'Aguanno, M. Bertolotti, M. J. Bloemer, C. M. Bowden, and I. Nefedov, Phys. Rev. E **60**, 4891 (1999).
[8] Y. Dumeige, P. Vidakovic, S. Sauvage, I. Sagnes, J. A. Levenson, C. Sibilia, M. Centini, G. D'Aguanno, and M. Scalora, Appl. Phys. Lett. **78**, 3021 (2001).
[9] P. Lalanne and H. Benisty, J. Appl. Phys. **89**, 1512 (2001).
[10] M. Le Vassor d'Yerville, E. Centeno, D. Cassagne, and J. P. Albert, Proc. SPIE **5450**, 181 (2004).
[11] J. M. Pottage, E. Silvestre, and P. S. Russell, J. Opt. Soc. Am. A **18**, 442 (2001).
[12] J. A. Armstrong, N. Bloembergen, J. Ducuing, and P. S. Pershan, Phys. Rev. **127**, 1918 (1962).
[13] R. Reinisch and M. Nevière, Phys. Rev. B **26**, 5987 (1982).
[14] V. Berger, Phys. Rev. Lett. **81**, 4136 (1998).

[15] A. R. Cowan and J. F. Young, Phys. Rev. B **65**, 085106 (2002).
[16] J. P. Mondia, H. M. van Driel, W. Jiang, A. R. Cowan, and J. F. Young, Opt. Lett. **28**, 2500 (2003).
[17] A. M. Malvezzi, G. Vecchi, M. Patrini, G. Guizzetti, L. C. Andreani, F. Romanato, L. Businaro, E. Di Fabrizio, A. Passaseo, and M. De Vittorio, Phys. Rev. B **68**, 161306(R) (2003).
[18] H. Schmidt, A. C. Abare, J. E. Bowers, S. P. Denbaars, and A. Imamoglu, Appl. Phys. Lett. **75**, 3611 (1999).
[19] D. Coquillat, J. Torres, D. Peyrade, R. Legros, J. P.Lascaray, M. Le Vassor d'Yerville, E. Centeno, D. Cassagne, J. P. Albert, Y. Chen, and R. M. De La Rue, Opt. Express **12**, 1097 (2004).
[20] D. Peyrade, Y. Chen, L. Manin Ferlazzo, A. Lebib, N. Grandjean, D. Coquillat, R. Legros, and J. P. Lascaray, Microelectron. Eng. **57-8**, 843 (2001).
[21] J. Torres, D. Coquillat, R. Legros, J. P. Lascaray, F. Teppe, D. Scalbert, D. Peyrade, Y. Chen, O. Briot, M. Le Vassor d'Yerville, E. Centeno, D. Cassagne, and J. P. Albert, Phys. Rev. B **69**, 085105 (2004).
[22] D. M. Whittaker and I. S. Culshaw, Phys. Rev. B **60**, 2610 (1999).
[23] M. Nevière, E. Popov, and R. Reinisch, J. Opt. Soc. Am. A **12**, 513 (1995).
[24] The very details of the nonlinear calculation procedure will be given elsewhere.
[25] A. Yariv, *Optical Electronics* (Saunders, Philadelphia, 1991).
[26] J. Miragliotta, D. K. Wickenden, T. J. Kistenmacher, and W. A. Bryden, J. Opt. Soc. Am. B **10**, 1447 (1993).
[27] Y. R. Shen, *The Principles of Nonlinear Optics* (Wiley, New York, 1984).